Supplementary material

Table of contents

S1 Methods

S1.1 Surface element analysis

X-ray photoelectron spectroscopy (XPS) analysis was performed with an Axis Ultra DLD instrument (Kratos Analytical, Manchester, UK), using monochromatic AlKα radiation (1486.6 eV), operated at 20 mA and 10 kV. Survey spectra were recorded with a pass energy of 160 eV, a dwell time of 500 ms, and a resolution of 1 eV, while C 1s detail scans were obtained with a pass energy of 20 eV, a dwell time of 259.7 ms, and a resolution of 0.1 eV, with three sweeps per measurement cycle. The take-off angle was 0° and ultra-high vacuum during measurement was 4×10^{-7}Pa. For measurement, the MAOM fraction was fixed on a sample bar with carbon conductive tape (Agar Scientific Elektron Technology UK Ltd., Stansted, UK) with an area of about 15 mm^2. Per sample, three spots were measured, comprising an area of 300 × 700 µm each in the slot modus. For charge compensation the neutralizer was active during measurement, however, complete compensation was not possible and the survey spectra were corrected relative to the Si 2p peak at a binding energy of 103 eV (Si-O bond, Okada et al., 1998; Woche et al., 2017). Survey spectra were quantified with the software Vision 2 (Kratos Analytical, Manchester, UK), using a linear baseline and the implemented relative sensitivity factors. Carbon speciation was performed with the software CasaXPS (Version 2.318PR1.0, Casa Software Ltd., UK) by defining four peaks with respect to the C oxidation state, (C1) O=C-O, O=C-N at 289.3 eV; (C2) C=O, O-C-O at 287.9 eV; (C3) C-O, C-N at 286.4 eV; and (C4) C-C, C-H at 284.8 eV (Gerin et al., 2003). Carbon species were further assigned to the following groups: (C1) carbon with three bonds to oxygen and/or nitrogen as in carboxyl and amides (O=C-O, O=C-N), (C2) carbon with two bonds to oxygen as in aldehydes and ketones (C=O, O-C-O), (C3) carbon with a single bond to oxygen or nitrogen as in carbohydrates and amines (C-O, C-N), and (C4) carbon with bonds to carbon or hydrogen as in aliphatic and aromatic compounds (C=C, C-C, C-H) (Gerin et al., 2003; Poggenburg et al., 2018). The peak shapes were symmetric with a Gauss/Lorentz ratio of 85/15, using a linear baseline. The full width at half maximum (FWHM) was constrained between 1.4 and 1.8 eV (Gerin et al., 2003) and the peak position was allowed to vary by ± 0.5 eV. The content of all detected elements is given in atom% and fitting results are given as percentage of total peak area.

S2 Tables

Table S1. Standard substances for the EA-IRMS measurements

Substance	Company
Quartz sand* (Blank)	In-house standard
High organic sediment (HOS)	IVA Analysetechnik, Meerbusch, Germany (In-house)
USGS 25	IAEA**
Cellulose	IAEA**
Caffeine	IAEA**
N1	IAEA**
N2	IAEA**
$CaCO_3$	In-house standard
Needle litter	In-house standard

*Washed with HCl and glowed at 1040°C
**International Atomic Energy Agency, Seibersdorf Laboratory, Vienna, Austria

Table S2. Contents of dithionite- and oxalate-extractable Fe (Fe_d resp. Fe_o) and oxalate-extractable Al (Al_o) and Mn (Mn_o). Extractions were conducted for the samples from the first sampling in November 2016. Data show the mean (n = 6) with the standard deviation in brackets.

Depth increment [cm]	**Fe_d [mg g^{-1}]**	**Fe_o [mg g^{-1}]**	**Al_o [mg g^{-1}]**	**Mn_o [mg g^{-1}]**
0-5	2.38 (0.21)	1.03 (0.22)	0.56 (0.16)	0.29 (0.31)
5-10	2.42 (0.66)	1.13 (0.53)	0.50 (0.10)	0.05 (0.04)
10-20	2.71 (0.33)	1.51 (0.33)	0.64 (0.18)	0.14 (0.20)
20-30	2.42 (0.36)	1.22 (0.22)	1.05 (0.21)	0.38 (0.43)
30-40	2.11 (0.25)	0.95 (0.14)	1.31 (0.23)	0.58 (0.43)
40-50	1.87 (0.21)	0.75 (0.09)	1.08 (0.13)	0.51 (0.37)
50-60	1.70 (0.16)	0.60 (0.11)	0.94 (0.11)	0.53 (0.18)
60-70	1.65 (0.33)	0.51 (0.14)	0.64 (0.11)	0.61 (0.17)
70-80	1.84 (0.89)	0.45 (0.18)	0.48 (0.16)	0.54 (0.16)
80-90	1.68 (0.62)	0.40 (0.20)	0.38 (0.13)	0.70 (0.24)
90-100	1.65 (0.70)	0.40 (0.22)	0.35 (0.13)	0.58 (0.18)
100-120	1.99 (1.14)	0.49 (0.36)	0.40 (0.20)	0.68 (0.33)
120-140	2.47 (1.88)	0.60 (0.51)	0.41 (0.25)	0.57 (0.37)
140-160	2.04 (2.12)	0.42 (0.49)	0.29 (0.26)	0.57 (0.25)
160-180	1.15 (0.83)	0.23 (0.18)	0.16 (0.08)	0.89 (0.24)

Table S3. Surface element composition of the MAOM fraction, including a set of the most common elements in soil in at%, derived from quantification of XPS survey spectra. Traces of W were remnants of density fractionation, using sodium polytungstate (SPT). Data show the mean of three replicate measurements per sample, SD in brackets.

Plot	Depth [cm]	O	C	N	Na	K	Ca	Mg	W	Fe	Al	Si
1	0-5	51.36 (1.59)	27.32 (2.74)	1.07 (0.08)	0.56 (0.05)	0.05 (0.02)	0.01 (0.02)	0.03 (0.03)	0.07 (0.03)	0.29 (0.14)	2.00 (0.08)	17.24 (1.31)
	5-10	55.84 (0.41)	21.03 (1.02)	0.75 (0.06)	0.61 (0.08)	0.13 (0.04)	0.01 (0.02)	0.07 (0.01)	0.03 (0.01)	0.54 (0.11)	2.34 (0.15)	18.66 (0.43)
	10-20	58.50 (0.85)	16.72 (1.38)	0.63 (0.08)	0.92 (0.08)	0.23 (0.04)	0.02 (0.03)	0.00 (0.01)	0.05 (0.03)	0.91 (0.09)	3.57 (0.15)	18.45 (0.90)
	20-30	59.43 (0.66)	15.82 (0.78)	0.62 (0.14)	0.81 (0.10)	0.12 (0.04)	0.07 (0.02)	0.11 (0.12)	0.07 (0.02)	1.22 (0.06)	4.82 (0.25)	16.91 (0.35)
	30-40	57.13 (0.60)	20.04 (0.22)	0.92 (0.22)	0.45 (0.12)	0.06 (0.05)	0.03 (0.05)	0.15 (0.10)	0.28 (0.04)	1.34 (0.25)	5.96 (0.70)	13.65 (0.52)
	40-50	56.51 (2.84)	20.64 (3.99)	0.83 (0.06)	0.46 (0.02)	0.06 (0.03)	0.08 (0.05)	0.00 (0.00)	0.34 (0.03)	1.53 (0.13)	6.43 (0.34)	13.13 (0.91)
	100-120	64.78 (0.56)	7.17 (0.53)	0.17 (0.10)	1.11 (0.04)	0.48 (0.10)	0.14 (0.03)	0.34 (0.11)	0.19 (0.01)	1.94 (0.27)	7.41 (0.35)	16.27 (0.36)
	120-140	64.82 (0.51)	7.37 (0.64)	0.02 (0.04)	0.90 (0.07)	0.28 (0.02)	0.12 (0.04)	0.32 (0.03)	0.11 (0.01)	1.97 (0.19)	6.02 (0.50)	18.06 (0.47)
2	0-5	51.45 (4.38)	29.20 (7.09)	1.06 (0.04)	0.50 (0.20)	0.06 (0.06)	0.03 (0.03)	0.02 (0.02)	0.00 (0.00)	0.26 (0.10)	1.77 (0.28)	15.65 (2.71)
	5-10	48.53 (3.45)	32.42 (1.86)	0.85 (0.39)	0.90 (0.21)	0.16 (0.06)	0.00 (0.00)	1.13 (1.95)	0.00 (0.00)	0.54 (0.32)	2.89 (0.33)	12.58 (0.49)
	10-20	57.44 (1.99)	18.68 (1.67)	0.75 (0.28)	0.79 (0.14)	0.10 (0.06)	0.00 (0.00)	0.19 (0.29)	0.00 (0.00)	0.74 (0.16)	2.85 (0.43)	18.46 (0.90)
	20-30	58.98 (0.75)	18.14 (0.89)	0.82 (0.25)	0.77 (0.08)	0.04 (0.01)	0.01 (0.01)	0.00 (0.00)	0.05 (0.05)	1.20 (0.13)	4.50 (0.15)	15.49 (0.11)
	30-40	55.30 (0.72)	24.03 (1.18)	1.05 (0.18)	0.45 (0.08)	0.02 (0.02)	0.03 (0.05)	0.00 (0.00)	0.26 (0.03)	1.22 (0.09)	5.72 (0.09)	11.92 (0.64)
	40-50	58.47 (0.59)	18.35 (1.80)	0.86 (0.04)	0.45 (0.11)	0.02 (0.03)	0.00 (0.00)	0.01 (0.01)	0.27 (0.05)	1.33 (0.28)	5.84 (1.00)	14.39 (3.01)
	100-120	64.65 (0.38)	8.98 (0.25)	0.47 (0.09)	1.20 (0.06)	0.30 (0.05)	0.18 (0.04)	0.04 (0.08)	0.17 (0.05)	1.72 (0.11)	7.30 (0.47)	15.00 (0.28)
	120-140	64.55 (0.20)	9.23 (0.32)	0.19 (0.18)	0.93 (0.10)	0.26 (0.04)	0.11 (0.04)	0.00 (0.00)	0.09 (0.01)	1.85 (0.21)	5.72 (0.22)	17.08 (0.10)
3	0-5	55.02 (3.32)	24.17 (4.44)	1.04 (0.33)	0.65 (0.25)	0.05 (0.03)	0.00 (0.00)	0.00 (0.00)	0.03 (0.02)	0.19 (0.18)	1.62 (0.66)	17.24 (2.20)
	5-10	55.95 (4.68)	22.67 (5.77)	0.85 (0.20)	0.72 (0.15)	0.04 (0.03)	0.06 (0.06)	0.37 (0.37)	0.03 (0.03)	0.72 (0.15)	2.49 (0.23)	16.10 (2.17)
	10-20	55.70 (1.71)	22.24 (2.27)	0.96 (0.14)	0.69 (0.03)	0.02 (0.02)	0.06 (0.06)	0.00 (0.00)	0.12 (0.03)	0.95 (0.23)	3.71 (0.09)	15.56 (1.07)
	20-30	52.21 (3.75)	27.61 (6.43)	1.06 (0.16)	0.45 (0.15)	0.00 (0.00)	0.03 (0.05)	0.03 (0.03)	0.17 (0.03)	1.05 (0.14)	4.93 (0.58)	12.47 (1.91)
	30-40	54.39 (2.70)	25.55 (3.79)	0.97 (0.25)	0.47 (0.06)	0.04 (0.03)	0.00 (0.00)	0.00 (0.00)	0.24 (0.02)	1.20 (0.23)	5.46 (0.36)	11.69 (0.63)
	40-50	59.54 (0.62)	17.00 (1.23)	0.90 (0.05)	0.61 (0.10)	0.07 (0.05)	0.06 (0.05)	0.00 (0.00)	0.24 (0.03)	1.28 (0.07)	6.71 (0.40)	13.59 (0.59)
	100-120	64.05 (1.24)	9.96 (1.08)	0.26 (0.14)	1.03 (0.09)	0.21 (0.04)	0.11 (0.10)	0.00 (0.00)	0.16 (0.04)	1.60 (0.31)	6.75 (0.13)	15.85 (0.66)
	120-140	64.93 (2.26)	7.82 (3.49)	0.28 (0.25)	0.99 (0.21)	0.21 (0.05)	0.11 (0.10)	0.00 (0.00)	0.10 (0.02)	2.18 (0.08)	6.13 (0.43)	17.25 (1.52)

S3 Figures

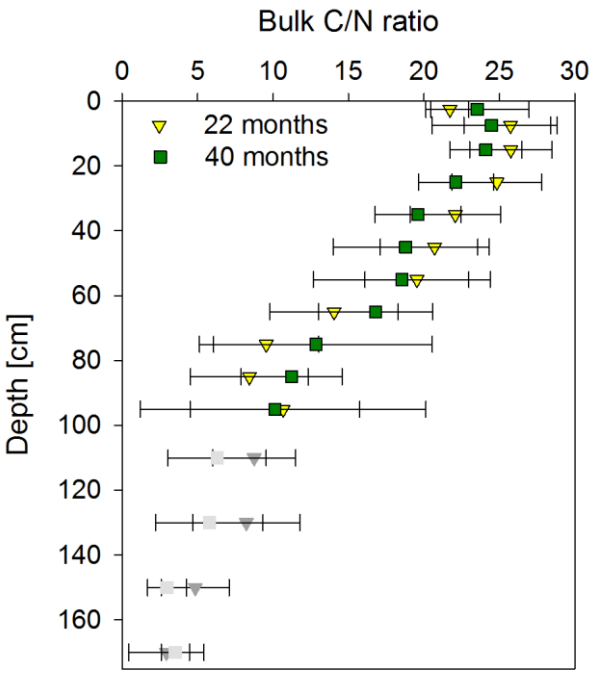

Figure S1. Mean C/N ratio of the bulk soil from both sampling times, 22 months and 40 months after labeled litter application. Data show the mean of 6 samples and error bars show the standard deviation. The y-axis shows the mean depth of each soil increment. Nitrogen contents in samples below 100 cm were increasingly below the detection limit and not reliable, therefore C/N ratios are marked in grey.

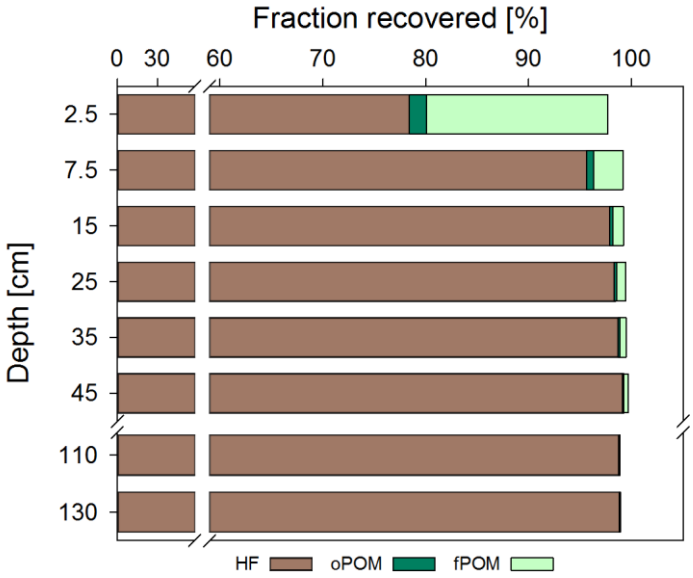

Figure S2. Mean mass recovery and fraction distribution of the soil density fractions heavy fraction (HF), occluded particulate organic matter (oPOM), and free particulate organic matter (fPOM) as the mean of both sampling times (November 2016 and May 2018). The y-axis shows the mean depth of each soil increment. Bars show the mean of 12 samples, the standard deviation varied for HF between 0.3-15 %, for oPOM between 0.1-1.6 %, and for fPOM between 0.1-18 %. Please note that for better visibility, both axes have breaks.

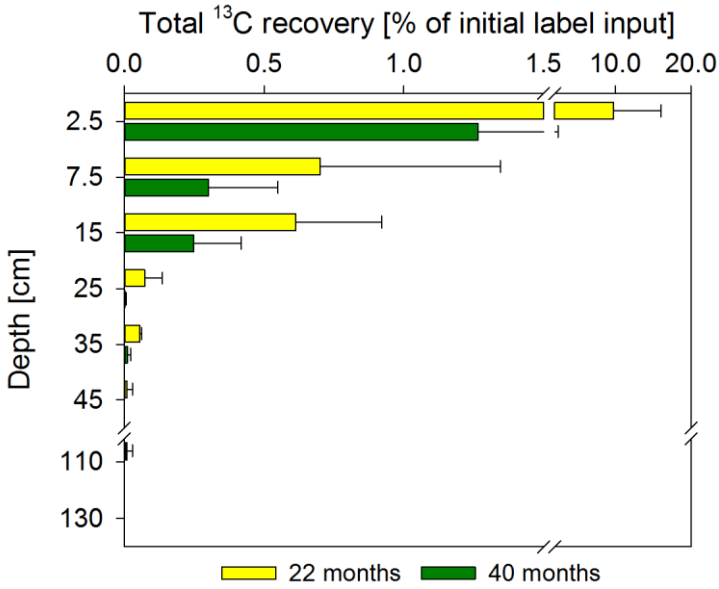

Figure S3. Mean ^{13}C recovered at each sampling time, 22 months and 40 months after labeled litter application, in % of the initial label input (n = 3). Bars show the sum of all fractions per depth increments, error bars depict the standard deviation. According to ANOVA analysis, there were no significant differences ($p > 0.05$) in the total recovered ^{13}C per depth increment between both sampling times, except of the depth 30-40 cm ($p = 0.004$). Please note that for better visibility, both axes have breaks.

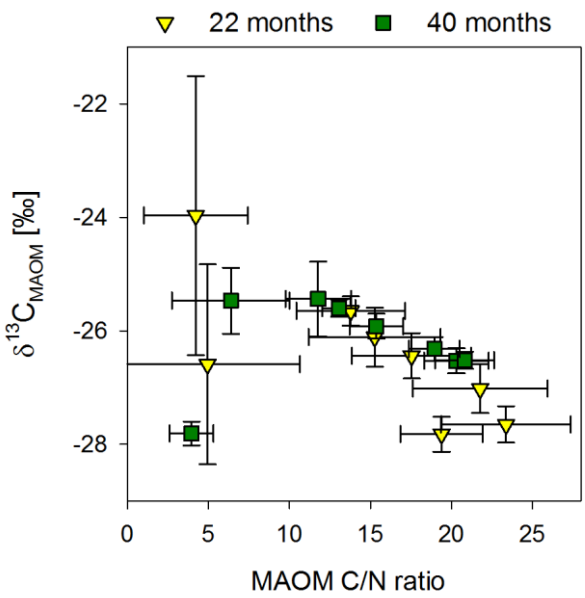

Figure S4. Correlation of the ^{13}C abundance of the mineral-associated organic matter (MAOM) controls on the Y-axis and the corresponding C/N ratio on the X-axis from both sampling times, 22 months and 40 months after labeled litter application. Data show the mean of three replicates, error bars depict the standard deviation. Spearman correlation resulted in a significant negative correlation for both variables for the first sampling in November 2016 ($r = -0.677$, $p < 0.05$) and the second sampling in May 2018 ($r = -0.883$, $p < 0.05$).

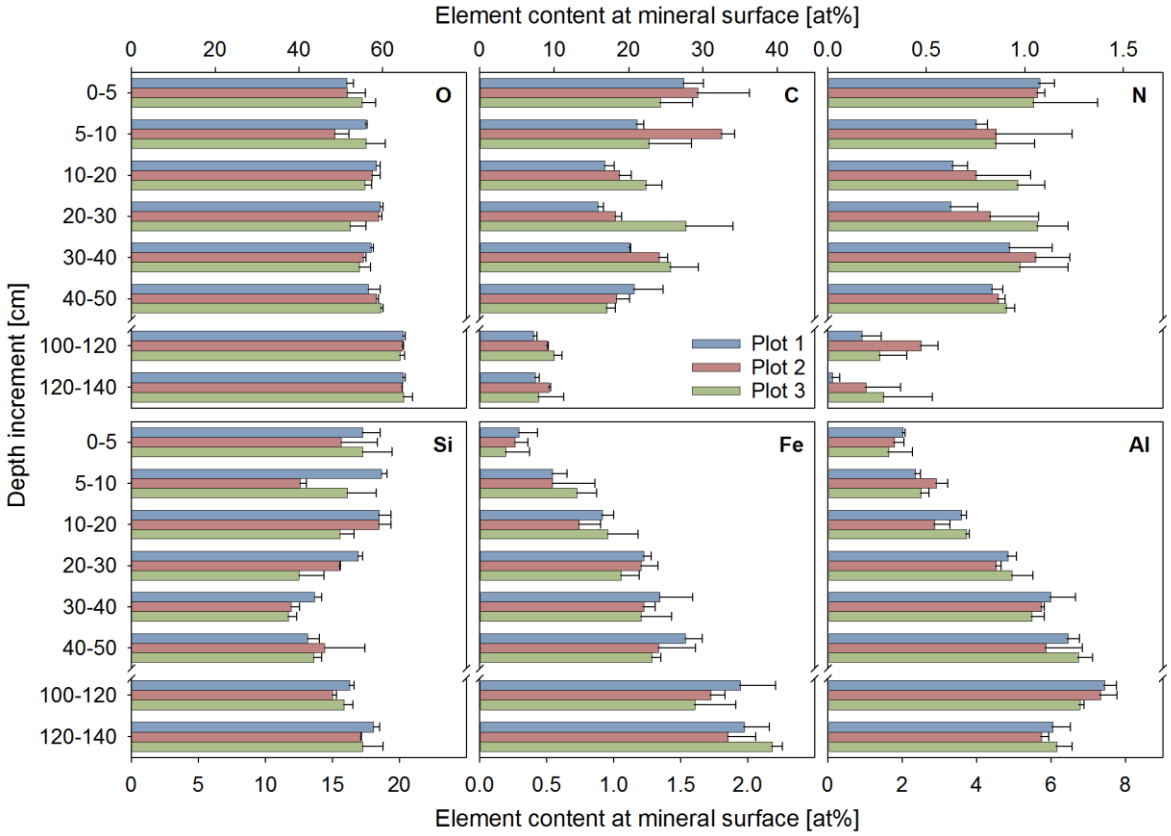

Figure S5. Contents of selected elements on the heavy fraction (HF) mineral surface layer according to XPS analysis. Bars show the mean of three spots measured per sample per plot and depth increment, error bars represent the standard deviation. Please note that the X-axis have different scales.

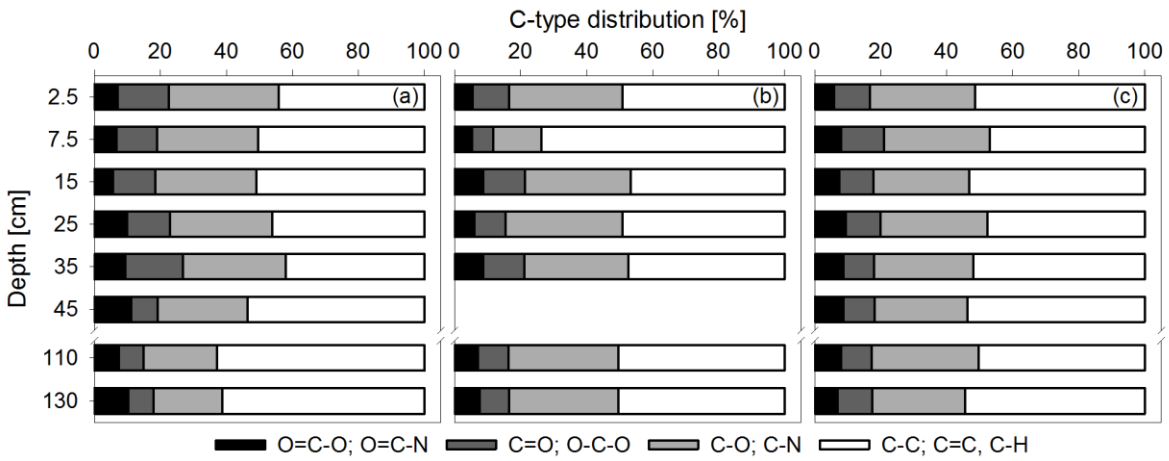

Figure S6. Distribution of carbon species of the mineral-associated organic matter (MAOM) fraction with depth of plot 1 (a), plot 2 (b), and plot 3 (c), derived from XPS C1s detail scans in percent of the total peak area. Carbon species were divided according to the C oxidation state and further assigned to the following groups: carboxyl and amides (O=C-O, O=C-N), aldehydes and ketones (C=O, O-C-O), carbohydrates and amines (C-O, C-N), and aliphatic and aromatic compounds (C=C, C-C, C-H).

S4 References

Gerin, P.A., Genet, M.J., Herbillon, A.J., Delvaux, B., 2003. Surface analysis of soil material by X-ray photoelectron spectroscopy. Eur. J. Soil Sci. 54, 589–604. https://doi.org/10.1046/j.1365-2389.2003.00537.x

Kögel-Knabner, I., 2002. The macromolecular organic composition of plant and microbial residues as inputs to soil organic matter. Soil Biol. Biochem. 34, 139–162. https://doi.org/10.1016/S0038-0717(01)00158-4

Okada, K., Kameshima, Y., Yasumori, A., 1998. Chemical Shifts of Silicon X-ray Photoelectron Spectra by Polymerization Structures of Silicates. J. Am. Ceram. Soc. 81, 1970–1972. https://doi.org/10.1111/j.1151-2916.1998.tb02579.x

Poggenburg, C., Mikutta, R., Schippers, A., Dohrmann, R., Guggenberger, G., 2018. Impact of natural organic matter coatings on the microbial reduction of iron oxides. Geochim. Cosmochim. Acta 224, 223–248. https://doi.org/10.1016/j.gca.2018.01.004

Woche, S.K., Goebel, M.-O., Mikutta, R., Schurig, C., Kaestner, M., Guggenberger, G., Bachmann, J., 2017. Soil wettability can be explained by the chemical composition of particle interfaces - An XPS study. Sci. Rep. 7, 42877. https://doi.org/10.1038/srep42877